Revista Mexicana de Astronomía y Astrofísica, **50**, 145–150 (2014)

THE STRONG/WEAK SHOCK TRANSITION IN CYLINDRICAL AND PLANAR BLAST WAVES

A. C. Raga,[1] J. Cantó,[2] A. Rodríguez-González,[1] and A. G. Petculescu[3]

Received 2013 November 14; accepted 2014 January 29

RESUMEN

Un fuerte episodio de formación estelar puede tener como consecuencia la producción de hasta $\sim 10^3$ estrellas masivas, las cuales después de unos $\sim 10^6$ yr tendrán explosiones de supernova. Dependiendo de la distribución espacial de las supernovas, su efecto combinado producirá ondas de choque con distintas geometrías. En este artículo, derivamos una solución para supernovas que explotan a lo largo de una distribución lineal (por ejemplo, a lo largo de un sector de brazo espiral) y también discutimos el caso de una distribución plana. Finalmente, comparamos los resultados obtenidos para una distribución con concentración central, una distribución lineal y una distribución plana.

ABSTRACT

A strong burst of star formation can result in the formation of up to $\sim 10^3$ massive stars, which after a time of $\sim 10^6$ yr will have supernova explosions. Depending on the spatial distribution of the supernovae, their combined effect will produce blast waves with different geometries. In this paper, we derive a solution for supernovae going off in a linear distribution (e.g., along a sector of a spiral arm) and also discuss the case of a planar distribution. Finally, we compare the results obtained for a centrally concentrated, a linear and a planar distribution for the supernovae.

Key Words: galaxies: halos — ISM: clouds — stars: formation

1. INTRODUCTION

Star formation bursts can lead to the formation of up to $\sim 10^5 - 10^6$ stars, of which $\sim 500 - 5000$ can be massive stars with supernova explosions at the end of their evolution, producing a SN rate of ~ 0.5-100 supernovas per yr (Aretxaga et al. 1990). The collection of supernovae explosions within a limited spatial region will lead to the formation of a common, expanding hot bubble (see, e.g., Chevalier & Clegg 1985). Once the high supernova rate (resulting from the starburst) is over, the hot bubble will expand, driving a blast wave pushed by the combined energy of all the supernovae.

In this paper we explore the effect of the geometrical distribution of the supernovae on the expanding blast wave. We explore three basic possibilities:

1. a centrally concentrated SN distribution (basically corresponding to the standard, Taylor-Sedov solution with the combined energy of all of the supernovae),
2. a linear distribution of SNs,
3. a planar SN distribution.

A linear distribution of SN explosions (item 2, above) will produce a cylindrical blast wave. Such a blast wave can be modeled analytically with the same methods that yield the solution of a spherical blast wave. A planar SN distribution can also be modeled analytically.

The self-similar expansion of strong, cylindrical blast waves was studied by Pittard et al. (2001). This paper includes the additional effect of a spatially extended mass loading term (representing evaporation from dense, embedded clouds).

In this work, we use the model of Chernyi (1957) with the extension to weak shocks of Raga et al. (2012) to model a cylindrical (§§ 2–5) and a planar

[1]Instituto de Ciencias Nucleares, Universidad Nacional Autónoma de México, Mexico.
[2]Instituto de Astronomía, Universidad Nacional Autónoma de México, Mexico.
[3]Department of Physics, Univ. of Louisiana at Lafayette, USA.

blast wave (§ 6). We then compare the general properties of spherical, cylindrical and planar blast wave solutions (§ 7). The results are summarized in § 8.

2. CHERNYI'S APPROXIMATION

The expansion of a spherical blast wave was studied by Taylor (1946, 1950) and by Sedov (1959), who found a full analytic solution for the structure of the flow variables within the expanding bubble. Inspired by the fact that the spherical blast wave flow has a hot, low density interior surrounded by a much denser shell (in approximate pressure equilibrium with the interior), Chernyi (1957) proposed a simplified model of these two components.

In this model (described in detail in the books of Zel'dovich & Raizer 1967, and Dyson & Williams 1980), one assumes that the energy of the supernova is transformed into thermal energy of the internal, low mass, hot bubble and kinetic energy of the outer, thin shell (which incorporates most of the mass of the swept-up environment). Requiring pressure balance between the hot bubble and the post-strong shock, swept-up shell material one obtains a differential equation for the radius of the blast wave, which agrees very well with the solution of Sedov (1959).

Raga et al. (2012) realized that Chernyi's (1957) model could be generalized to the case of an outer shock with the full strong/weak jump conditions, and that the resulting differential equation for the expanding hot bubble also had an analytic solution. Interestingly, this analytic solution is very similar to the expansion law used by Tang & Wang (2005) to fit the results obtained from numerical blast wave simulations.

In the following sections, we first derive in detail the strong/weak blast wave version of Chernyi's model for a cylindrical blast wave (§§ 3–5), and then describe the solution for the case of a planar blast wave (§ 6).

3. THE DIVISION OF THE ENERGY OF THE EXPLOSION INTO THERMAL (BUBBLE) AND KINETIC (SHELL) ENERGIES

Following the derivation of Dyson & Williams (1980), we assume that the energy per unit length of the cylindrical explosion ϵ is divided into thermal energy of the expanding, hot bubble and kinetic energy of the outer, thin shell:

$$\epsilon = \frac{P}{\gamma - 1} A + \frac{1}{2} m_s v_s^2 \,, \tag{1}$$

where γ is the specific heat ratio, $A = \pi r^2$ is the cross sectional area of the expanding hot bubble (r being its outer cylindrical radius), m_s is the mass (per unit length) and v_s the velocity of the swept-up material in the thin, outer shell.

Now, assuming that the outer shock is strong, the shock velocity v_c is

$$v_c = \frac{\gamma + 1}{2} v_s \,, \tag{2}$$

and its pressure is

$$P_s = \frac{2}{\gamma + 1} \rho_0 v_c^2 \,, \tag{3}$$

where ρ_0 is the density of the (homogeneous) environment. The mass (per unit length) of the cylindrical shell is:

$$m_s = \rho_0 A_c \,, \tag{4}$$

where $A_c = \pi r_c^2$ is the area subtended by the outer shock wave. Considering the different velocities of the outer shock wave and of the expanding shell (see equation 2), we find that the areas subtended by the outer radius of the bubble (A) and by the shock wave (A_c) follow the relation

$$A_c = \left(\frac{\gamma + 1}{2} \right)^2 A \,. \tag{5}$$

Now, setting $P_s = P$ and combining equations (1−5) one obtains the relation

$$\epsilon = \Gamma \pi r^2 P \,; \quad \Gamma \equiv \frac{3 + \gamma^2}{4(\gamma - 1)} \,, \tag{6}$$

between the cylindrical radius r and the pressure P of the hot bubble.

We should note that the dependence of Γ on the specific heat ratio γ in equation (6) differs from the one obtained by Raga et al. (2012, who modeled spherical blast waves) because these authors set $A_c = A$ (instead of using equation 5). These two different estimates of the Γ constant, however, lead to very similar expanding bubble solutions.

Following Raga et al. (2012), we will assume that the fraction of the energy ϵ of the explosion which ends up as thermal energy of the hot bubble (i.e., equation 6, derived assuming a strong outer shock) is also valid in the regime in which the shock is no longer strong (see § 4). The error introduced by this inconsistency in the model is, however, less important than the errors introduced by neglecting the thermal energy and the momentum of the outer shell.

4. THE EQUATION OF MOTION FOR THE OUTER RADIUS OF THE BUBBLE

We now consider the general (strong/weak) shock jump relations:

$$P_s = \frac{2}{\gamma+1}\rho_0 v_c^2 - \frac{\gamma-1}{\gamma+1}P_0\,, \tag{7}$$

$$v_{ps} = \frac{\gamma-1}{\gamma+1}v_c + \frac{2}{\gamma+1}\frac{c_0^2}{v_c}\,, \tag{8}$$

where P_s is the post-shock pressure and v_{ps} the post-shock velocity in the shock reference frame. The shock moves at a velocity v_c, and $P_0 = \rho_0 c_0^2/\gamma$ is the environmental pressure (with ρ_0 and c_0 being the environmental density and sound speed, respectively).

Also, the "piston relation" between the shock velocity v_c the post-shock velocity v_{ps} and the outward velocity of the shell material v_s is:

$$v_s = v_c - v_{ps}\,. \tag{9}$$

Combining equations (8–9) and considering that $dr/dt = v_s$ (where r is the outer radius of the hot bubble) we obtain:

$$\frac{1}{c_0}\frac{dr}{dt} = \frac{2}{\gamma+1}\left(\frac{v_c}{c_0} - \frac{c_0}{v_c}\right)\,. \tag{10}$$

We now rewrite equation (7) in the form:

$$\left(\frac{v_c}{c_0}\right)^2 = \frac{\gamma+1}{2\rho_0 c_0^2}\left(P + \frac{\gamma-1}{\gamma+1}P_0\right)\,, \tag{11}$$

and combine it with equation (6) to obtain:

$$\left(\frac{v_c}{c_0}\right)^2 = \frac{1}{2\gamma}\left[(\gamma+1)\left(\frac{r_f}{r}\right)^2 + \gamma - 1\right]\,, \tag{12}$$

with

$$r_f \equiv \sqrt{\frac{\gamma\epsilon}{\Gamma\rho_0 c_0^2}}\,. \tag{13}$$

From equation (12) it is clear that for $r \to r_f$ the velocity of the expanding bubble has the limit $v_c \to 0$. It is therefore clear that r_f (defined by equation 13) is the maximum radius attained by the hot bubble as it reaches pressure balance with the surrounding environment.

Finally, combining equations (10) and (12) we obtain the equation of motion for the outer radius r of the hot bubble:

$$\frac{1}{c_0}\frac{dr}{dt} = \frac{2}{\gamma+1}\times \left[\sqrt{\frac{\gamma+1}{2\gamma}\left(\frac{r_f}{r}\right)^2 + \frac{\gamma-1}{2\gamma}} - \frac{1}{\sqrt{\frac{\gamma+1}{2\gamma}\left(\frac{r_f}{r}\right)^2 + \frac{\gamma-1}{2\gamma}}}\right]\,. \tag{14}$$

The "strong shock" and the general solutions to this equation are discussed in § 5 and § 6, respectively. Once this equation has been integrated, the radius of the outer shock r_c can be found as a function of the bubble radius r by integrating the differential equation

$$\frac{dr_c}{dr} = \frac{1}{2}\frac{(\gamma+1)(r_f/r)^2 + \gamma - 1}{(r_f/r)^2 - 1}\,, \tag{15}$$

which can be derived from equations (10) and (14).

5. THE STRONG SHOCK SOLUTION

The strong shock solution can be derived by taking the $r \ll r_c$ of equation (14), from which one obtains:

$$\frac{1}{c_0}\frac{dr}{dt} = \sqrt{\frac{2}{\gamma(\gamma+1)}}\frac{r_f}{r}\,, \tag{16}$$

which can be straightforwardly integrated to obtain the radius r of the hot bubble as a function of time:

$$r = \left[\sqrt{\frac{2}{\gamma(\gamma+1)}}2c_0 r_f\, t\right]^{1/2} = 2\left[\frac{2(\gamma-1)\epsilon}{(\gamma+1)(3+\gamma^2)\pi\rho_0}\right]^{1/4} t^{1/2}\,, \tag{17}$$

where for the second equality we have also used equations (6) and (13).

The $r \gg r_f$ limit of equation (15) direcly gives a radius for the outer shock wave

$$r_c = \frac{\gamma+1}{2}r\,, \tag{18}$$

which is consistent with equation (5). Therefore, in the initial, strong shock regime, the radii of the hot bubble and of the outer shock both evolve as a function of time following a $t^{1/2}$ power law. This solution is shown in Figure 1.

6. THE GENERAL SOLUTION

Equation (14) has the analytic integral:

$$t = \frac{r_f}{c_0}\left[F(x) - F(0)\right]\,, \tag{19}$$

with

$$x = \sqrt{\frac{2\gamma}{\gamma+1}}\frac{r}{r_f}\,, \tag{20}$$

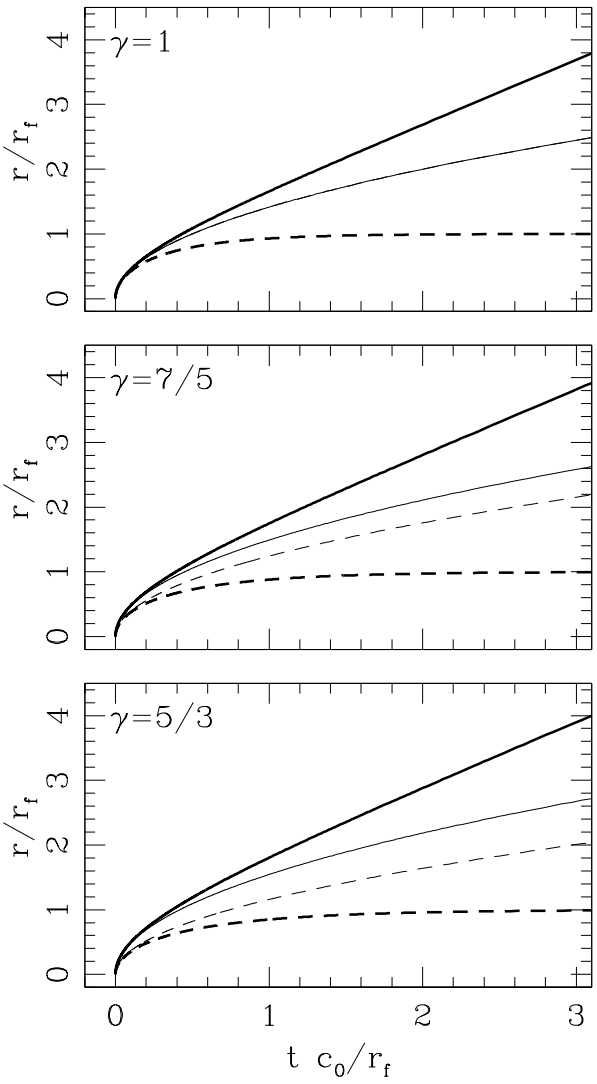

Fig. 1. The radius of the blast wave (solid lines) and the outer radius of the hot bubble (dashed lines) as a function of time. The thin lines correspond to the strong shock solution (equations 17 and 18) and the thick lines to the general, stong/weak shock solution (equations 19–22). The top frame shows the radii obtained for a specific heat ratio $\gamma = 1$, the central frame for $\gamma = 7/5$, and the bottom frame for $\gamma = 5/3$. We should note that for $\gamma = 1$ the blast wave and hot bubble radii coincide in the strong shock case, since the shock compression is infinite.

and

$$F(x) = \gamma \left[\tanh^{-1}(y) - y \right] ,$$

with

$$y \equiv \frac{\sqrt{\gamma+1}}{2\gamma} \sqrt{2\gamma + (\gamma-1)x^2} \, . \qquad (21)$$

Equations (19−21) give the time-dependent radius of the hot bubble in an implicit way.

The equation for the radius r_c of the shock wave (equation 15) can also be integrated analytically, to obtain:

$$r_c = \frac{r_f}{2} \left[\gamma \ln \left(\frac{1 + r/r_f}{1 - r/r_f} \right) - (\gamma - 1) \frac{r}{r_f} \right] . \qquad (22)$$

The hot bubble and shock radii calculated with equations (19−22) are shown in Figure 1.

Comparing the strong shock (thin lines in Figure 1) and the general strong/weak shock solution (thick lines) one sees that:

- the outer radius of the hot bubble (dashed lines) asymptotically goes to the pressure equilibrium radius r_f in the general solution, but continues to grow for increasing times in the strong shock solution,
- the velocity of the blast wave asymptotically tends to the environmental sound speed in the general solution, and tends to zero in the strong shock solution.

We should note again (see the last paragraph of § 3) that the assumption that the energy of the SN explosion is divided (in constant fractions) between the thermal energy of the hot bubble and the kinetic energy of the dense shell is incorrect at later evolutionary times (in particular, in the final configuration described in the first of the two items above). This inconsistency is at the heart of the "thick shell" formalism of Raga et al. (2012). However, these authors find that (at least for the spherical blast wave) the "thick shell" formalism still agrees qualitatively well with numerical solutions of the Euler equations for large evolutionary times. This agreement is a result of the fact that in the full solutions (of the Euler equations) a fraction ∼1 of the initial energy of the SN explosion remains in the form of thermal energy of the hot bubble, and only a small fraction of the SN energy is in the form of kinetic energy of the dense shell at all evolutionary times. This fact is reproduced by equation (6), which gives a fraction of the SN energy of $1 - (\gamma-1)^{-1}\Gamma^{-1} \sim 0.2 \rightarrow 0.3$ for $\gamma = 7/5 \rightarrow 5/3$ in the form of kinetic energy of the dense shell.

7. THE EXPANSION OF A PLANAR BLAST WAVE

In this section we consider the case of an explosion with a planar energy distribution e (energy per unit area). In a completely analogous way to the derivation of § 3−§ 4, one can find an equation of motion for the distance z (from the "explosion plane"

to the edge of the hot bubble) of the form:

$$\frac{\gamma+1}{2c_0}\frac{dz}{dt} = \sqrt{\frac{\gamma+1}{2\gamma}\frac{z_f}{z} + \frac{\gamma-1}{2\gamma}} - \frac{1}{\sqrt{\frac{\gamma+1}{2\gamma}\frac{z_f}{z} + \frac{\gamma-1}{2\gamma}}}\,, \tag{23}$$

where

$$z_f \equiv \frac{\gamma e}{2\Gamma\rho_0 c_0^2}\,, \tag{24}$$

with Γ given by equation (6).

Equation (23) has an analytic integral which gives an increasing z vs. t dependence, with an asymptotic limit $z \to z_f$ for $t \to \infty$. It is also possible to derive an equation of motion for the shock (equivalent to the cylindrical shock equation 15), which also has an analytic solution.

8. CARPET BOMBING

Let us assume that we have a large number of supernovae going off at approximately the same time, adding to a total energy E. If the supernovae are distributed in a centrally concentrated region, the flow produced by the combined explosions can be approximated by the spherical blast wave solution. Raga et al. (2012) showed that such a spherical blast wave leaves behind a hot bubble of pressure equilibrium with a radius

$$R_f = \left(\frac{3}{4\pi}\frac{\gamma E}{\Gamma\rho_0 c_0^2}\right)^{1/3}\,, \tag{25}$$

with Γ given by equation (6).

If the supernovae have a uniform linear spatial distribution with a total length $L \gg r_0 f$ (with r_f given by equation 13), we can model the resulting flow with the cylindrical blast wave solution of § 3−§ 4 with an energy per unit length $\epsilon = E/L$. This solution leaves behind a cylindrical pressure equilibrium bubble with cylindrical radius

$$r_f = \left(\frac{\gamma E}{\pi\Gamma\rho_0 c_0^2 L}\right)^{1/3}\,. \tag{26}$$

Finally, if the supernovae have a uniform distribution on an $L \times L$ planar surface with $L \gg z_f$ (see equation 24), the final pressure equilibrium bubble has a height

$$z_f \equiv \frac{\gamma E}{2\Gamma\rho_0 c_0^2 L^2}\,, \tag{27}$$

above the plane of the SN distribution.

The fact that the models assume that a fixed fraction of the supernova energy ends up as thermal energy of the hot bubble (see § 3) directly leads to the result that the volume of the final, pressure equilibrium hot bubble has the value

$$V_f = \frac{4\pi}{3}R_f^3 = \pi r_f^2 L = 2 z_f L^2 = \frac{\gamma E}{\Gamma\rho_0 c_0^2}\,, \tag{28}$$

regardless of the geometry of the spatial distribution of the supernovae.

On the other hand, the surface area of the final hot bubble has values

$$\begin{aligned} A_{\rm sp} &= 4\pi R_f^2 = 4\pi\left(\frac{3}{4\pi}V_f\right)^{2/3}; \\ A_{\rm cyl} &= 2\pi r_f L = 2\sqrt{\pi V_f L}; \\ A_{\rm pl} &= 2L^2, \end{aligned} \tag{29}$$

for the spherical, cylindrical and planar cases. In the cylindrical and planar cases, the surface area has been computed in the $L \gg r_f$, z_f limit (for which these cases are applicable, see above).

From this we see that while the volume of the final hot bubble (V_f, see equation 28) is independent of the geometry of the SN spatial distribution, the surface area of the hot bubble is not. In the cases of the linear and planar SN distribution, it is possible to increase the surface area of the hot bubble by spreading the supernovae thinly (along the axis or axes of the distribution). Such spread out distributions will result in larger surface areas for the hot bubbles, which will promote more efficient mixing with the surrounding material.

9. SUMMARY

We have derived an analytic solution for an expanding, cylindrical blast wave with the transition from the strong to the weak shock regime (§ 3−§ 6). A similar solution can be derived for a planar blast wave (§ 7). These solutions are relevant for astrophysical situations in which a large number of supernovae go off in a limited time interval and in a limited spatial region, as would be obtained from a star formation burst with many massive stars (e.g., in nuclear starbursts in Seyfert galaxies, see Aretxaga et al. 1990).

If we have a centrally concentrated star formation burst, the combined effect of the supernovae that will go off will produce an approximately spherical blast wave. This blast wave will leave behind a spherical hot bubble. This flow is similar to the single supernova model described by Raga et al. (2012), but with an energy corresponding to the combined energy of all the supernovae.

In a star formation burst occuring along a sector of a spiral arm, we would expect an approximately

linear spatial distribution of supernovae. Such a distribution of supernovae would produce an approximately cylindrical blast wave that would leave behind a cylindrical hot bubble in pressure equilibrium with the surrounding environment.

In a star formation burst with a planar distribution, the resulting supernovae will produce an approximately planar blast wave. This blast wave would leave behind a hot slab (in pressure equilibrium with the surrounging environment).

While in these three cases (spherical, linear or planar supernovae distributions) the resulting hot bubbles have the same volume, in the cases of linear or planar spatial distributions it is possible to obtain much larger surface areas for the hot bubbles. These larger surface areas will result in:

- an increased amount of mixing with the surrounding environment,
- the potential for producing larger amounts of induced star formation in surrounding regions.

Therefore, while a centrally concentrated distribution of supernovae will produce hot bubbles which will rise in the stratified ISM of the parent galaxy before mixing with their environment (see Rodríguez-González & Raga 2013), a linear or a planar SN distribution will result in more local mixing. Such effects might be relevant for the redistribution of metals produced in star bursts within galaxies.

We conclude by noting that the calculations described above are based on non-radiative blast wave models. The transition to a radiative, momentum conserving phase at later evolutionary times (see, e.g., Blinnikov, Imshennik, & Utrobin 1982; Falle 1981) will clearly modify the behaviour of the flows.

The cylindrically symmetric strong/weak blast wave solution derived in this paper also has possible applications to geophysical flows (related to lightning) and to laboratory experiments. For example, most interesting laser-generated plasma experiments producing approximately cylindrical blast waves have been recently described by Smith et al. (2007) and Symes et al. (2010). We will attempt a future comparison of our model with these experiments.

We acknowledge support from the Conacyt grants 101356, 101975, 165584, 167611 and 167625, and the DGAPA-UNAM grants IN105312 and IN106212.

REFERENCES

Aretxaga, I., Díaz, A. I., Terlevich, R., & Terlevich, E. 1990, Ap&SS, 171, 61
Blinnikov, S. I., Imshennik, V. S., & Utrobin, V. P. 1982, Soviet Astron. Lett., 8, 361
Chernyi, G. G. 1957, Dokl. Akad. Nauk SSSR, 112, 213
Chevalier, R. A., & Clegg, A. W. 1985, Nature, 317, 44
Dyson, J. E., & Williams, D. A. 1980, The Physics of the Interstellar Medium (Manchester: Manchester Univ. Press)
Falle, S. A. E. G. 1981, MNRAS, 195, 1011
Pittard, J. M., Dyson, J. E., & Hartquist, T. W. 2001, Ap&SS, 278, 269
Raga, A. C., Cantó, J., Rodríguez, L. F., & Velázquez, P. F. 2012, MNRAS, 424, 2522
Rodríguez-González, A., & Raga, A. C. 2013, RevMexAA, 49, 171
Sedov, L. I. 1959, Similarity and Dimensional Methods in Mechanics (New York: Academic Press)
Symes, D. R., et al. 2010, High Energy Density Physics, 6, 274
Smith, R. A., Lazarus, J., Hohenberger, M., Moore, A. S., Robinson, J. S., Gumbrell, E. T., & Dunne, M. 2007, Ap&SS, 307, 131
Tang, S., & Wang, Q. D. 2005, ApJ, 628, 205
Taylor, G. I. 1946, Proc. R. Soc. London Ser. A, 186, 273
_____. 1950, Proc. R. Soc. London Ser. A, 201, 159
Zel'dovich, Ya. B., & Raizer, Yu. P. 1967, Physics of Shock Waves and High-Temperature Hidrodynamic Phenomena, (New York: Academic Press)

J. Cantó: Instituto de Astronomía, Universidad Nacional Autónoma de México, Apdo. Postal 70-264, 04510 México, D.F., Mexico.
A. G. Petculescu: Department of Physics, University of Louisiana at Lafayette, USA (andi@louisiana.edu).
A. C. Raga and A. Rodríguez-González: Instituto de Ciencias Nucleares, Universidad Nacional Autónoma de México, Apdo. Postal 70-543, 04510 México, D.F., Mexico (raga, ary@nucleares.unam.mx).